Diabetologia (2015) 58:1282–1290
DOI 10.1007/s00125-015-3568-x

ARTICLE

Bone morphogenetic protein 4 inhibits insulin secretion from rodent beta cells through regulation of calbindin1 expression and reduced voltage-dependent calcium currents

Gitte L. Christensen[1] · Maria L. B. Jacobsen[1] · Anna Wendt[2] · Ines G. Mollet[2] · Josefine Friberg[1] · Klaus S. Frederiksen[3] · Michael Meyer[4] · Christine Bruun[5] · Lena Eliasson[2] · Nils Billestrup[1]

Received: 20 November 2014 / Accepted: 4 March 2015 / Published online: 2 April 2015
© Springer-Verlag Berlin Heidelberg 2015

Abstract

Aims/hypothesis Type 2 diabetes is characterised by progressive loss of pancreatic beta cell mass and function. Therefore, it is of therapeutic interest to identify factors with the potential to improve beta cell proliferation and insulin secretion. Bone morphogenetic protein 4 (BMP4) expression is increased in diabetic animals and BMP4 reduces glucose-stimulated insulin secretion (GSIS). Here, we investigate the molecular mechanism behind this inhibition.

Methods BMP4-mediated inhibition of GSIS was investigated in detail using single cell electrophysiological measurements and live cell Ca^{2+} imaging. BMP4-mediated gene expression changes were investigated by microarray profiling, quantitative PCR and western blotting.

Results Prolonged exposure to BMP4 reduced GSIS from rodent pancreatic islets. This inhibition was associated with decreased exocytosis due to a reduced Ca^{2+} current through voltage-dependent Ca^{2+} channels. To identify proteins involved in the inhibition of GSIS, we investigated global gene expression changes induced by BMP4 in neonatal rat pancreatic islets. Expression of the Ca^{2+}-binding protein calbindin1 was significantly induced by BMP4. Overexpression of calbindin1 in primary islet cells reduced GSIS, and the effect of BMP4 on GSIS was lost in islets from calbindin1 (*Calb1*) knockout mice.

Conclusions/interpretation We found BMP4 treatment to markedly inhibit GSIS from rodent pancreatic islets in a calbindin1-dependent manner. Calbindin1 is suggested to mediate the effect of BMP4 by buffering Ca^{2+} and decreasing Ca^{2+} channel activity, resulting in diminished insulin exocytosis. Both BMP4 and calbindin1 are potential pharmacological targets for the treatment of beta cell dysfunction.

Keywords Beta cells · BMP4 · *Calb1* · Calbindin1 · Diabetes · Exocytosis · Insulin secretion

Electronic supplementary material The online version of this article (doi:10.1007/s00125-015-3568-x) contains peer-reviewed but unedited supplementary material, which is available to authorised users.

✉ Lena Eliasson
Lena.Eliasson@med.lu.se

✉ Nils Billestrup
Billestrup@sund.ku.dk

[1] Department of Biomedical Sciences, University of Copenhagen, Nørre Alle 20, 2100 Copenhagen, Denmark

[2] Lund University Diabetes Center, Lund University, CRC 91-11, Jan Waldenströms gata 35 SUS Malmö, 205 02 Malmö, Sweden

[3] Biopharmaceuticals Research Unit, Novo Nordisk A/S, Måløv, Denmark

[4] Department of Cellular Physiology, Ludwig Maximilian University of Munich, Munich, Germany

[5] Department of Incretin and Islet Biology, Novo Nordisk A/S, Måløv, Denmark

Abbreviations

BMP	Bone morphogenetic protein
ECM	Extracellular matrix
FDR	False discovery rate
GSIS	Glucose-stimulated insulin secretion
HBSS	Hanks' balanced salt solution
KO	Knockout
VDCC	Voltage-dependent Ca^{2+} channel
WT	Wild type

Introduction

Pancreatic beta cells initially compensate for insulin resistance by increasing their mass and activity to maintain normal blood glucose levels [1]. In individuals who progress to develop type 2 diabetes, beta cells eventually fail to adapt and progressive loss of functional beta cells starts [1]. Although current type 2 diabetes drugs targeting insulin resistance or insulin secretion are initially efficient, beta cell mass and function tend to decline over time [2, 3]. Unidentified factors may limit the ability of the beta cells to adapt to insulin resistance. In our search for factors with inhibitory effects on beta cells, we recently described the inhibition of beta cell proliferation and insulin secretion by bone morphogenetic protein 4 (BMP4) [4].

BMPs belong to the TGF-β protein family, members of which are known to play central roles in pancreas and islet development [5–10]. While the role of BMPs in the developing pancreas and beta cells has gained much attention [8, 11, 12], less is known about their function in the postnatal pancreas. There is increasing evidence that BMP2/4 are inflammatory markers in various tissues under diabetic conditions [13–15]. We recently showed that BMP2/4 are expressed in pancreatic islets and upregulated during diabetes progression in islets from *db/db* mice and by proinflammatory cytokines in vitro [4]. Although the culture of pancreatic islets in the presence BMP2/4 negatively affects beta cell function, it appears that the effect of BMPs in vivo is more complex. Beta cell specific deletion of BMP receptor 1A (*Bmpr1a*) resulted in impaired glucose-stimulated insulin secretion (GSIS), whereas *BMP4* transgene overexpression increased GSIS [16]. In contrast, deficiency of inhibitor of differentiation 1 (*Id1*), encoding a central BMP-regulated transcription factor, resulted in enhanced insulin secretion and protection from diet-induced glucose intolerance, suggesting that BMPs and ID1 normally inhibit adult beta cell function [17]. BMPs are both released from and affect several metabolically relevant tissues, including fat, liver and kidney, thus adding to the complexity of the role of BMPs in metabolism [14, 18, 19]. To characterise the direct effects of BMPs on beta cells, we recently reported BMP4-mediated inhibition of beta cell proliferation and repression of GSIS from mouse, rat and human islets [4]. Here, we further characterise the effects of BMP4 on insulin secretion using single cell electrophysiological measurements, and evaluate gene regulation to identify the molecular mechanism for the observed inhibition of insulin secretion.

Methods

Rat islet isolation and culture

Neonatal rat islets of Langerhans were isolated from 4-day-old Wistar rat pups (Taconic, Lille Skensved, Denmark), as previously described [20]. All mice were housed according to the Principles of Laboratory Care. The isolated islets were pre-cultured for 7–10 days in RPMI 1640 with UltraGlutamine (Lonza, Vallensbaek, Denmark) and supplemented with 10% newborn calf serum (Biological Industries, Kibbutz Beit Haemek, Israel), 100 U/ml penicillin and 100 μg/ml streptomycin (Gibco, Life Technologies, Taastrup, Denmark) in 5% CO_2 at 37°C. For experiments, rat islets were cultured as intact and free-floating in medium supplemented with 2% human serum (BioWhittaker, Lonza) or as single cells following digestion with 0.2% trypsin (Gibco) and 10 mmol/l EDTA (Gibco) in Hanks' balanced salt solution (HBSS). Dispersed islets were cultured on coverslips coated with bovine corneal extracellular matrix (ECM; Biological Industries) in the medium described above containing 2% human serum.

Mouse islet isolation and culture

Pancreatic islets from 10–12-week-old female NMRI mice were isolated by collagenase digestion, as previously described [21]. Islets were handpicked into albumin-coated Petri dishes (1 mg albumin/ml HBSS) and cultured for 1 day in medium I (RPMI 1640 containing 10 mmol/l glucose and 10% FCS, 100 U/ml penicillin, and 100 μg/ml streptomycin) and then for a further 3 days in medium II (RPMI 1640 containing 10 mmol/l glucose and 2% FCS, 100 U/ml penicillin, and 100 μg/ml streptomycin) in the absence or presence of BMP4 (50 ng/ml). After culture, mouse islets were fixed for transmission electron microscopy (see electronic supplementary material (ESM) Fig. 1 for further details) or dispersed into single cells using Ca^{2+}-free buffer for electrophysiological experiments.

Pancreatic islets from 12–19-week-old 129SV/C57/6crl wild type (WT) and calbindin1 (*Calb1*) knockout (KO) mice (calbindin$^{D28k-/-}$) [22] were isolated by bile duct perfusion of the pancreas with Liberase (Roche, Hvidovre, Denmark). Digestion was stopped by the addition of HBSS buffer containing Mg^{2+} and Ca^{2+} (Gibco), 3 g/l BSA and 0.5 g/l D-glucose. Islets were filtered through a 400 μm mesh, followed by 100 μm and 70 μm mesh strainers (BD Falcon, Albertslund, Denmark). Retained islets were handpicked under a dissection microscope and cultured for 1 day in medium I. The following day, islets were transferred to medium II, in which they were kept throughout stimulation. Female mice were used for electrophysiological experiments and male mice for insulin secretion assays.

Microarray analysis

A total of 800 intact, free-floating rat islets were cultured in 5.5 cm Petri dishes for 5–10 days and then exposed to BMP4 for 96 h. Total RNA was extracted using TRIzol (Gibco). One

microgram of total RNA was labelled using a One-Cycle Target labelling kit (Affymetrix, Santa Clara, CA, USA) following the manufacturer's instructions. Hybridisation cocktails were hybridised to Rat Genome 230 2.0 GeneChip arrays (Affymetrix) at 45°C for 17 h (at 60 rpm) in a Hybridization Oven 640 (Affymetrix). GeneChips were then washed and stained in a GeneChip fluidics station 450 using the EukGE-WS2v5_450 fluidics protocol (Affymetrix), and then scanned in a GeneChip scanner 3000 (Affymetrix). Microarray data were normalised and gene expression measures derived using the RMA algorithm and the 'Affy' Bioconductor package (www.bioconductor.org). A Custom chip definition file obtained from brainarray.mbni.med.umich.edu was used. Qlucore Omics Explorer 3.0 (Qlucore, Lund, Sweden) was used for statistical analysis of the normalised data. For comparing BMP4 to vehicle treatment, microarray data were variance filtered ($\sigma/\sigma(max)>0.1$), and the two groups compared using the Student's *t* test (false discovery rate [FDR]=5%; Benjamini Hochberg correction for multiple testing).

Analysis of *Calb1* and *Ins1* mRNA expression by real-time quantitative PCR

A total of 800 intact neonatal rat islets cultured for 5 days were exposed to 50 ng/ml BMP4 for the indicated time periods, and then total RNA was extracted using TRIzol. cDNA synthesis was performed using TaqMan Reverse Transcription Reagents (Applied Biosystems, Carlsbad, CA, USA). TaqMan Gene Expression probes against rat *Calb1* (Rn00583140_m1), *Ins1* (Rn02121433_g1) and *Ppia* (Rn_00690933_m1) were obtained from Applied Biosystems. Samples were run on an ABI PRISM 7900HT Sequence Detection System (Applied Biosystems). Each sample was run in duplicate or triplicate and expression was normalised to the internal control, *Ppia*.

Analysis of calbindin1 protein expression by western blotting

A total of 1,000 intact neonatal rat islets were cultured for 5–10 days prior to exposure to 50 ng/ml BMP4 for 24, 48, 72 or 96 h. SDS-PAGE and western blotting were performed as described previously [23]. Primary antibodies were rabbit anti-calbindin1 (Cell Signaling Technology, AH Diagnostics, Aarhus, DK) and mouse anti-β-actin (Abcam, Cambridge, UK). Chemiluminescence was detected using Lumi-GLO (Cell Signaling Technology) and visualised using Las 3000 (Fujifilm, GE Healthcare Europe, Brondby, Denmark). Densitometric scanning was performed using ImageJ freeware (National Institutes of Health, Bethesda, MD, USA).

GSIS

On day 7–10 after isolation, 40 neonatal rat islets were transferred to medium containing 2% human serum, 100 U/ml penicillin and 100 μg/ml streptomycin, and then stimulated with 50 ng/ml BMP4 for 0–96 h. Mouse islets were stimulated the day after isolation. For each condition, 20 islets were transferred to Krebs-Ringer HEPES buffer (KRHB; 115 mmol/l NaCl, 4.7 mmol/l KCl, 2.6 mmol/l $CaCl_2$, 1.2 mmol/l KH_2PO_4, 1.2 mmol/l $MgSO_4$, 10 mmol/l HEPES, 0.2% BSA, 2 mmol/l glutamine, 5 mmol/l $NaHCO_3$ and 1% each penicillin and streptomycin, pH 7.4) containing 2 mmol/l glucose and incubated for 90 min prior to the GSIS experiment. Islets were sequentially exposed to 2 mmol/l glucose, 20 mmol/l glucose, and 20 mmol/l glucose plus 10 μmol/l forskolin (Sigma-Aldrich, Brondby, Denmark) for 30 min. The buffer was then collected from each experimental group and insulin content was determined using an in-house insulin ELISA. Results were corrected for DNA content using Quant-IT PicoGreen dsDNA Reagent and Kit (Invitrogen, Life Technologies, Taastrup, Denmark).

Production of *Calb1* lentivirus

Mouse *Calb1* cDNA in the pENTR221 entry vector (Invitrogen) was transferred to the pLenti6.2/v5DEST Gateway vector (Invitrogen). Lentivirus was produced in HEK293ft cells using the ViraPower Lentiviral Expression System (Invitrogen, Carlsbad, CA, USA) and lentivirus particles were harvested by ultracentrifugation. Viral titer was determined in HT1080 cells (Invitrogen). The virus was used at a multiplicity of infection of 5 for 6 h.

Insulin release in single cells overexpressing calbindin1

Dispersed rat islet cells were cultured on coverslips coated with bovine corneal ECM in 4-well plates for 4 days prior to transduction with *Calb1*- or GFP-expressing lentivirus for 6 h at a MOI of 5. After 96 h, GSIS was evaluated as described above.

Electrophysiology

Capacitance measurements and ion current measurements were performed on single beta cells in a mixture of dispersed islets cells using the patch-clamp technique, as previously described [21]. Beta cells where identified by their size and the inactivation properties of the voltage-dependent Na^+ channel [24, 25]. Exocytosis was evoked by a train of 10 500 ms depolarisation events from −70 mV to 0 mV at a frequency of 1 Hz and measured as changes in membrane capacitance. The voltage-dependent Ca^{2+} channel (VDCC) current to voltage relationship was determined using a protocol in which the

membrane was depolarised from −70 mV to voltages between −40 mV and +40 mV for 50 ms.

Live cell Ca2$^+$ imaging

Islets were loaded with 4 μmol/l Fura-2-acetoxymethyl ester (TefLabs, Austin, TX, USA) for 40 min, followed by 30 min de-esterification in imaging buffer at pH 7.4 (3.6 mmol/l KCl, 0.5 mmol/l $MgSO_4$, 2.5 mmol/l $CaCl_2$, 140 mmol/l NaCl, 2 mmol/l $NaHCO_3$, 0.5 mmol/l NaH_2PO_3 and 5 mmol/l HEPES). High K^+ buffer was identical except for 70 mmol/l NaCl and 70 mmol/l KCl. Imaging was performed using a Polychrome V monochromator (TILL Photonics, Graefeling, Germany) and an Eclipse Ti Microscope (Nikon, Tokyo, Japan) with a ER-BOB-100 trigger on an iXON3 camera and iQ2 (Andor Technology, Belfast, UK) software. Recording was performed at 1 frame/s at 37°C under perfusion at 1 ml/min. A region was marked around each islet and the light intensity was recoded in that region to obtain the integrated light intensity per unit area (in μm^2) at 340 nm (150 ms exposure) and 380 nm (100 ms exposure). These measured intensities were then used to calculate the ratio of Fura-2 bound (340 nm) and unbound (380 nm) to Ca^{2+} at 1 frame/s.

Results

BMP4 inhibits GSIS

The effect of BMP4 on GSIS was investigated in neonatal rat islets. Pretreatment with 50 ng/ml BMP4 for 0–4 days resulted in a reduction in GSIS after 48 h (Fig. 1a). Acute stimulation with BMP4 (0 h) or pre-stimulation for up to 24 h had no effect on insulin secretion. In addition, doses as low as 2 ng/ml inhibit insulin secretion [4]. BMP4 stimulation had no effect on total islet insulin content (Fig. 1b) or *Ins1* mRNA levels (Fig. 1c). We did not observe any effect on the number, size or membrane proximity of insulin granules using high-resolution electron microscopy of adult mouse islets (ESM Fig. 1).

BMP4 inhibits exocytosis and VDCC current

The fact that BMP4 inhibits GSIS without affecting the total insulin content or total number of insulin granules suggests that BMP4 may target the secretory machinery. For a further detailed electrophysiological analysis of insulin secretion, we used dispersed primary mouse islet cells. We investigated exocytosis measured as increased membrane capacitance and found a reduced depolarisation-evoked increase in membrane capacitance in BMP4-treated primary mouse beta cells (Fig. 2a–e). The most pronounced effect was observed during depolarisation events 2–10 ('Depol 2–10'; Fig. 2d). This was

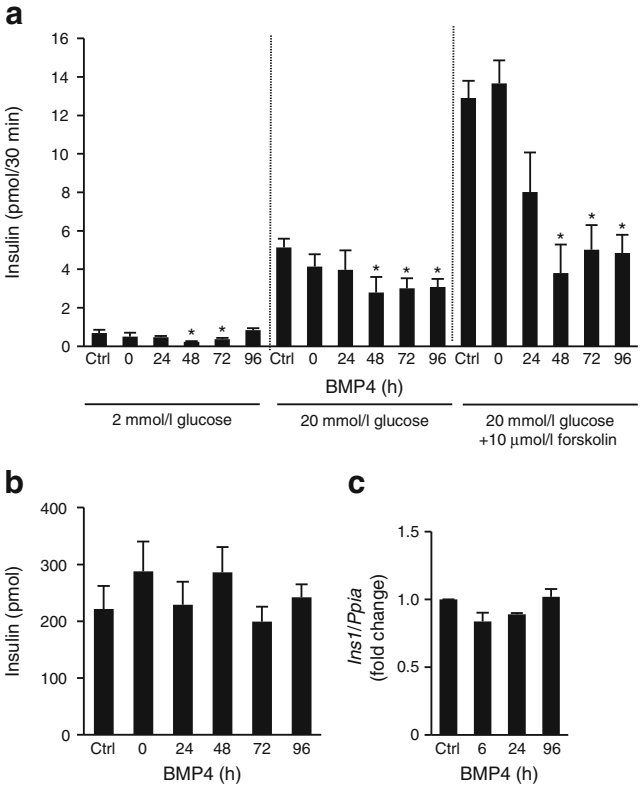

Fig. 1 BMP4 inhibits GSIS without affecting total insulin content. (**a**) Neonatal rat islets were pre-exposed to 50 ng/ml BMP4 for 0–96 h and GSIS was performed as described. (**b**) Post-assay insulin content of islets. DNA content was used for normalisation in (**a**) and (**b**). (**c**) A total of 800 intact neonatal rat islets were exposed to 50 ng/ml BMP4 for 0–96 h. Relative *Ins1* mRNA expression was normalised to *Ppia* expression. Data are mean ± SEM. Statistical significance was evaluated using ANOVA followed by Dunnett's *t* test. *$p < 0.05$

confirmed by a continued reduction in the exocytotic response to a second train of depolarisation events performed 2 min later (Fig. 2e). Exocytosis is highly dependent on Ca^{2+} influx through VDCCs [26]. We therefore determined the VDCC influx to voltage relationship (Fig. 2f, g). Beta cells exposed to BMP4 show ~50% reduced Ca^{2+} influx at 0 mV. BMP4 increased the Ca^{2+} sensitivity, i.e. increased the membrane capacitance per Ca^{2+} charge unit entering the cell, which suggests that the BMP4-dependent decrease in exocytosis is caused by a reduced Ca^{2+} current rather than a direct effect on exocytosis (Fig. 2h). Moreover, BMP4 may have a direct stimulatory effect on exocytosis that is less pronounced than the effect on the Ca^{2+} current.

To gain further insight into the mechanism of BMP4 inhibition of exocytosis, we performed live cell Ca^{2+} imaging of primary adult mouse islets. Evaluation of Ca^{2+} fluctuations was determined by differences in the Fura-2 340 nm:380 nm ratio (representative traces shown in Fig. 2i, j; all traces are shown in ESM Fig. 2). Temporal fluctuation of the intracellular Ca^{2+} in response to glucose were organised into two classes: class 1 islets have separate first and second phases, in

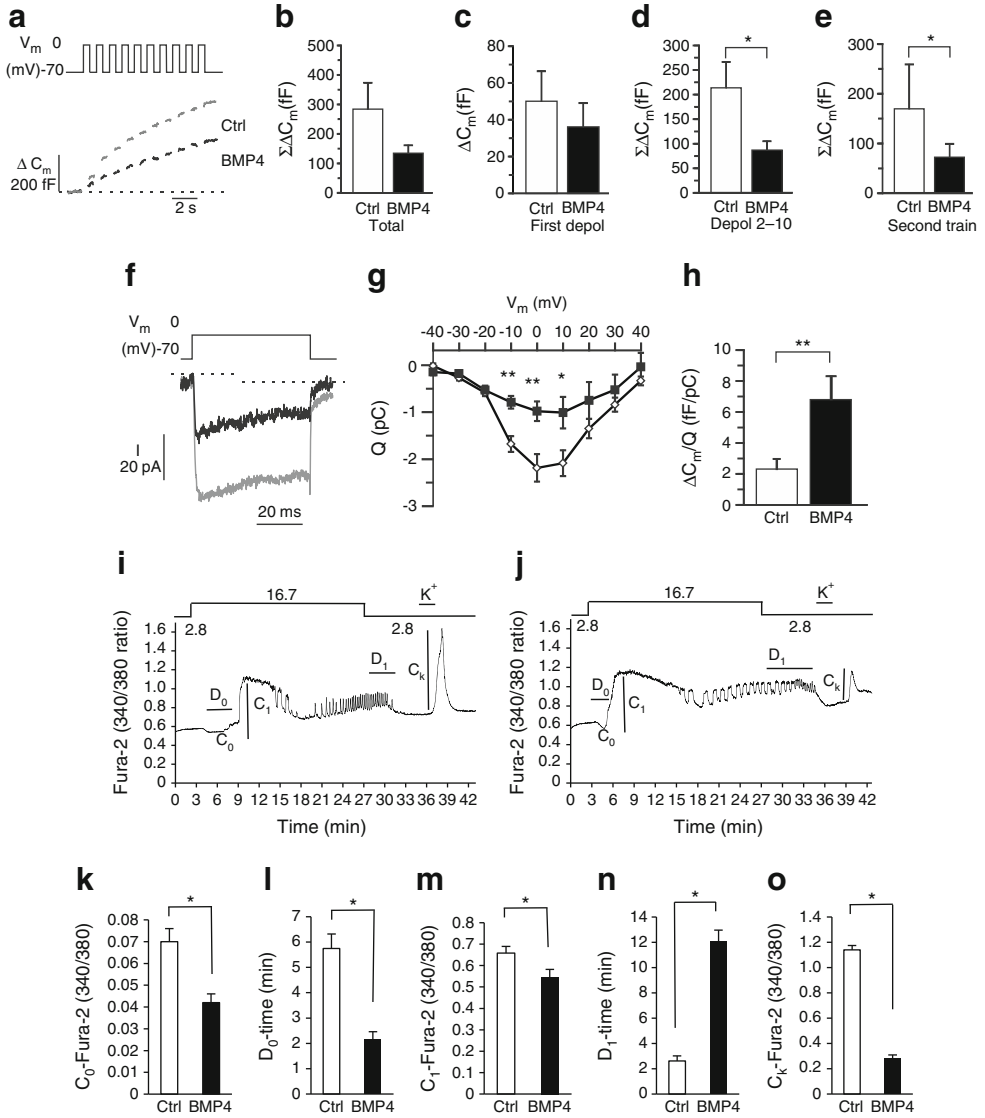

Fig. 2 BMP4 diminishes membrane capacitance increase and Ca^{2+} influx through VDCCs. (**a**) Example trace of depolarisation-induced exocytosis, measured as changes in cell membrane capacitance (ΔC_m) in a single mouse beta cell. (**b**) The mean increase in membrane capacitance evoked by a train of 10 depolarisation events, (**c**) the first depolarisation and (**d**) depolarisations 2–10. (**e**) Mean capacitance increase evoked by a second train applied 2 min later. (**f**) Example trace from a VDCC in a beta cell incubated in the absence (grey) and presence (black) of BMP4. (**g**) The measured charge (Q) as a function of the membrane voltage (V_m) during a 50 ms depolarisation. White diamonds, control cells; black squares, BMP4-treated cells. (**h**) The Ca^{2+} sensitivity of the exocytotic response measured as the capacitance increase during the first depolarisation event of the train (ΔC_m) shown in (**c**) divided by the Ca^{2+} influx (charge=Q) during the same 500 ms depolarisation. Data in (**b–e**) and (**g–h**) are mean ± SEM of n=9–16 experiments in each group. *$p<0.05$, **$p<0.01$. (**i**, **j**) Representative examples of a Ca^{2+} trace obtained from one islet pre-treated for 3 days with (**i**) vehicle (control) or (**j**) BMP4. C_0, Ca^{2+} dip occurring when 16.7 mmol/l glucose reaches the islets; D_0, time delay between 16.7 mmol/l glucose exposure and the first Ca^{2+} peak; C_1, amplitude of the first phase peak; D_1, time delay in response to low glucose; C_k, amplitude of high potassium peak. The staircase indicates the glucose concentrations of 2.8 mmol/l (2.8) and 16.7 mmol/l (16.7). The line with K^+ indicates the addition of 70 mmol/l KCl. Summary statistics of Ca^{2+} imaging traces shown for (**k**) C_0, (**l**) D_0, (**m**) C_1, (**n**) D_1 and (**o**) C_k. Ctrl, control; Depol, depolarisation

which a defined first phase peak is followed by a lowering of Ca^{2+} and a second phase with distinct regularly spaced Ca^{2+} oscillations; class 2 islets exhibit a rise in Ca^{2+} with no clear first and second phases and no distinct oscillations in the second phase. In all, 64% of control islets and 26% of BMP4-treated islets had a distinct first peak and second phase oscillations in the presence of high glucose (see ESM Table 1). In addition, there was a significant reduction in the first lowering of Ca^{2+} (Fig. 2j, k) and the first phase peak amplitude at 16.7 mmol/l glucose (Fig. 2j, m) and in the response to depolarising K^+ (Fig. 2j, o). The response time after increased glucose concentration was reduced by BMP4 treatment (Fig. 2j, l), whereas the response time to glucose lowering was increased

(Fig. 2n). We did not observe significant changes in the amplitude or frequency of Ca^{2+} oscillations.

BMP4 mediates upregulation of calbindin1

Since the effects of BMP4 on GSIS were first observed after 48 h exposure, we hypothesised that gene regulation is required for this effect. To unravel the mechanism of BMP4-mediated inhibition of GSIS we therefore performed a gene expression array comparing three independent sets of vehicle- and BMP4-treated neonatal rat islets (96 h). Using a FDR of 5%, we found 102 genes to be regulated by BMP4 (ESM Table 2). Genes up- or downregulated by more than twofold are shown in Table 1. Regulation of seven of these genes was verified in independent rat islet samples by q-pcr (denoted by [a] in Table 1).

We paid particular attention to genes known to be involved in hormone secretion and Ca^{2+} handling, based on the effects of BMP4 on insulin secretion, exocytosis and Ca^{2+} channel activity. We observed no regulation of BMP receptors or L-type Ca^{2+} channel subunits. One of the most strongly regulated genes was *Calb1*, which encodes an EF-hand Ca^{2+}-binding protein previously shown to regulate Ca^{2+} currents through VDCC and inhibit GSIS in beta cells [27–29]. BMP4 increased the expression of *Calb1* mRNA by sixfold in neonatal rat islets, resulting in a 2.5-fold increase in calbindin1 protein after 96 h (Fig. 3a,b) As shown in primary neonatal rat islets, BMP4 increased the expression of *Calb1* mRNA in adult mouse islets (Fig. 3c).

Table 1 Genes regulated by at least twofold in neonatal rat islets exposed to 50 ng/ml BMP4 for 96 h

Gene	Protein name	Fold change
Id3	DNA-binding protein inhibitor ID-3	17.92[a]
Id1	DNA-binding protein inhibitor ID-1	16.52[a]
Lypd8	Ly6/PLAUR domain containing protein 8 precursor	9.66
Irx-3	Iroquois-class homeodomain protein IRX-3	5.40
Calb1	Calbindin1	4.62[a]
Id2	DNA-binding protein inhibitor ID-2	4.25[a]
Micalcl	MICAL C-terminal-like protein	4.06
Fam101a	Family with sequence similarity 101. member A (Fam101a)	3.85
Lgals4	Galectin-4	3.72
Bambi	BMP and activin membrane-bound inhibitor homologue	3.25[a]
Atoh8	Protein atonal homologue 8	3.13
Arc	Activity-regulated cytoskeleton-associated protein	3.08
Mlph	Melanophilin	2.90
Camk1g	Calcium/calmodulin-dependent protein kinase type 1G	2.82
Chst10	Carbohydrate sulfotransferase 10	2.81
Dlk1	Protein delta homologue 1	2.75
Tppp3	Tubulin polymerisation-promoting protein family member 3	2.72
Tmem100	Transmembrane protein 100	2.68
Ckb	Creatine kinase B-type	2.63
Ppp1r36	Protein phosphatase 1 regulatory subunit 36	2.59
Tmem100	Transmembrane protein 100	2.51
Rtn4rl1	Reticulon-4 receptor-like 1	2.44
St5	Suppression of tumorigenicity 5 protein	2.34
Akap12	A-kinase anchor protein 12	2.30
Vash2	Vasohibin-2	2.20
Ddx31	Probable ATP-dependent RNA helicase DDX31	2.07
Fads1	Fatty acid desaturase 1	0.45
Nod3l	NOD3-like protein	0.44
Bmp3	Bone morphogenetic protein 3	0.43[a]
Htr5b	5-hydroxytryptamine (serotonin) receptor 5B	0.33
Gpr6	G protein-coupled receptor 6	0.28[a]

[a] Verified by quantitative PCR analysis of independent neonatal rat islet samples

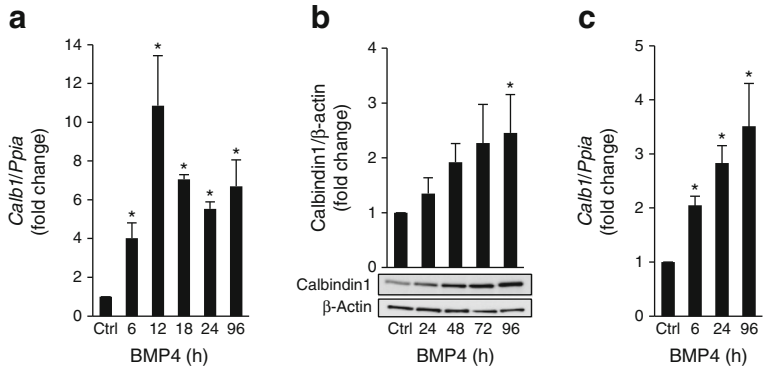

Fig. 3 BMP4 stimulates the expression of *Calb1*. Islets were stimulated with 50 ng/ml BMP4 for 0–96 h. (**a**) Relative *Calb1* mRNA expression in neonatal rat islets was normalised to *Ppia* expression. (**b**) Protein expression in neonatal rat islets was determined by western blotting using primary antibodies against calbindin1 and β-actin. A representative western blot is shown and densitometry quantification of three blots was performed in ImageJ. (**c**) Isolated mouse islets were stimulated with 50 ng/ml BMP4 for 0–96 h. Relative *Calb1* mRNA expression was normalised to *Ppia* expression. All data are mean ± SEM; n=3–4

Overexpression of *Calb1* impairs GSIS

To determine the role of calbindin1 in the BMP4-mediated effects on GSIS, we induced overexpression of *Calb1* in dispersed neonatal rat islet cells. Overexpression of *Calb1* significantly reduced GSIS (Fig. 4a). The transfection efficiency was more than 80%, resulting in a robust upregulation of calbindin1 protein (Fig. 4b).

BMP4 inhibition of GSIS and exocytosis is dependent on *Calb1* upregulation

We further investigated the effect of BMP4 on GSIS from pancreatic islets from *Calb1* KO mice and WT littermates. As for neonatal rat islets, we observed a significant inhibition of GSIS by BMP4 treatment in WT adult mouse islets (Fig. 4c), but none in islets from *Calb1* KO mice (Fig. 4c).

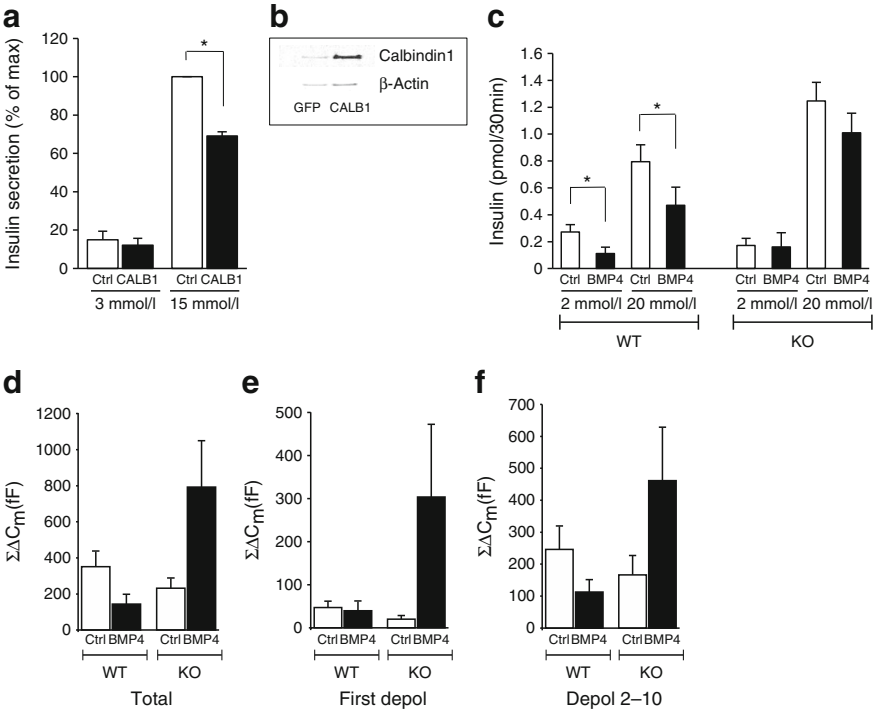

Fig. 4 Calbindin1 expression affects islet glucose and BMP4 responsiveness. (**a**) GSIS from dispersed neonatal rat islet cells overexpressing calbindin1 or GFP. Insulin secretion is depicted as % of control cells exposed to high glucose. (**b**) Western blot showing lentiviral overexpression of calbindin1. (**c**) Islets from *Calb1* knockout (KO) mice and littermate WT controls were exposed to 50 ng/ml BMP4 for 96 h and subsequently GSIS was determined, n=3. All data are mean ± SEM. (**d–f**) Mean increase in membrane capacitance evoked by (**d**) the full train, (**e**) the first depolarisation and (**f**) depolarisation events 2–10 in single mouse beta cells isolated from *Calb1* KO mice and littermate WT controls. CALB1, calbindin1; Ctrl, control; Depol, depolarisation; max, maximum. p<0.05 vs control

In accordance with this, BMP4 did not reduce exocytosis in islets from *Calb1* KO mice, but rather showed a nonsignificant increase in exocytosis (Fig. 4d–f).

Discussion

Here, we investigate the mechanism behind BMP4-mediated inhibition of GSIS in neonatal rat and adult mouse islets of Langerhans. This effect was not caused by reduced *Ins1* mRNA expression or protein content, or by changes in the number, size or localisation of insulin granules, but instead seems to be due to diminished Ca^{2+} influx through VDCCs resulting in reduced exocytosis. Metabolism of glucose increases intracellular ATP levels, resulting in closure of ATP-dependent K^+ channels and membrane depolarisation. Subsequent opening of VDCCs triggers Ca^{2+} entry which induces insulin exocytosis (reviewed in [30, 31]). Hence, Ca^{2+} entry is essential for the amount of insulin released. We observed a BMP4-dependent decrease in the VDCC current, leading to a reduction in depolarisation-induced exocytosis and GSIS. The Ca^{2+} sensitivity of exocytosis was not decreased but was instead increased, indicating that the reduced Ca^{2+} current is the main determinant of reduced exocytosis. Reduced Ca^{2+} influx was also confirmed by a lack of response to K^+ in live cell Ca^{2+} measurements. Both observations are indicative of reduced depolarisation-evoked Ca^{2+} influx or increased Ca^{2+} buffering after BMP4 treatment. An increase in Ca^{2+} buffering would agree with the continued and more pronounced reduction in late exocytosis evoked by the latter depolarisations and the second train (Fig. 2d, e). Interestingly, our microarray analysis identified *Calb1*, the gene encoding the Ca^{2+}-binding protein calbindin1, as being upregulated by BMP4. We confirmed this regulation in independent rat islet samples and mouse islets. Although it has been suggested that neonatal and adult islets respond differently to glucose and other stimuli, BMP4 inhibited GSIS and upregulated calbindin1 in both model systems. Overexpression of *Calb1* reduced GSIS. The effect of BMP4 on GSIS was lost in islets from *Calb1* KO mice (Fig. 4c). The exocytotic response to BMP4 in WT islets showed the same trend as previously observed (Figs 2a–e and 4d), whereas this regulation was lost in islets from *Calb1* KO mice. There was a trend towards increased exocytosis in response to BMP4 in *Calb1* KO mice, but this was nonsignificant and was not reflected in GSIS. BMP inhibition of GSIS was not observed in islets from *Calb1* KO mice, suggesting that increased calbindin1 expression may cause the observed BMP4-mediated decline in GSIS. Indeed, the BMP4-induced decrease in VDCC influx was remarkably similar to the effect observed upon overexpression of calbindin1 in a pancreatic beta cell line (Fig. 2b–h and [29]). In addition to a Ca^{2+}-scavenging effect, accumulating evidence suggests that calbindin1 reduces Ca^{2+} currents via an association with L-type VDDCs [29]. Glucose- and Ca^{2+}-dependent translocation of calbindin1 to the plasma membrane has previously been suggested to facilitate the interaction with L-type Ca^{2+} channels [28, 29]. This could explain the lack of effect on the capacitance increase evoked by the first depolarisation (Figs 2c and 4e), because the first influx of Ca^{2+} would induce translocation of calbindin1 to the plasma membrane.

Glucose-induced Ca^{2+} oscillations occur in fewer BMP4-treated islets compared with control cells, possibly because of reduced Ca^{2+} influx through VDCCs. This was further supported by the blunted Ca^{2+} response to high glucose and depolarising K^+ after BMP4 treatment (Fig. 3i–o and ESM Table 1). Loss of K^+-induced Ca^{2+} influx was also observed in a calbindin1-overexpressing cell line, indicating that this effect is caused by increased calbindin1 expression [27, 29]. Finally, Ca^{2+} oscillations persisted for longer in BMP4-treated islets when glucose was returned to 2.8 mmol/l (Fig. 2n and ESM Table 1), indicating a failure of the beta cells to repolarise to baseline. These data again suggest dysfunctional Ca^{2+} handling after BMP4 treatment.

Interestingly, calbindin1 expression is increased in pancreatic islets from diabetic rats and mice [32, 33]. Concomitant upregulation of BMP2 (but not BMP4) and calbindin1 in the islets of Langerhans has been observed in a type 2 diabetic mouse model [33]. BMP2 also upregulated the expression of calbindin1 and reduced GSIS in rat islets (data not shown). Generally, BMP2/4 may be considered as inflammatory markers in several metabolic tissues. Under diabetic conditions, expression of BMP2 or BMP4 has been reported to increase in the arteries, kidney, bones and islets [4, 14, 18, 19]. Increased BMP4 expression was reflected by increased circulating levels of BMP4 in type 2 diabetic patients in one study [13]. Thus, systemic inhibition of BMP2/4 appears to represent a possible strategy for broad targeting of a mediator of low-grade inflammation associated with type 2 diabetes. Interestingly, it was recently reported that systemic administration of the natural BMP inhibitor noggin lowered blood glucose levels in *db/db* mice [14].

In conclusion, we have provided insight into the mechanisms involved in BMP4-mediated inhibition of insulin secretion and gene regulation in islets of Langerhans, and identified calbindin1 as a mediator of BMP4-induced beta cell dysfunction.

Acknowledgements We acknowledge the technical assistance from H. Fjordvang and L.G. Pedersen from the University of Copenhagen, S. Mach from the Ludwig Maximilian University of Munich, and B.–M. Nilsson and A.-M. Veljanovska-Ramsay from the Lund University Diabetes Center.

Funding We are thankful for support from the Novo Nordisk Foundation, Danish Research Council, Danish Diabetes Academy, European Foundation for the Study of Diabetes, A.P. Møller Foundation, Swedish Research Council, Region Skåne (ALF), Albert Påhlsson Foundation and Swedish Diabetes Foundation. LE is a senior researcher at the Swedish

Research Council. GLC holds a postdoctoral grant from the Danish Diabetes Academy.

Duality of interest MLBJ, CB and KSF are employees of Novo Nordisk A/S.

Contribution statement NB, GLC, MLBJ, CB and LE designed the study; GLC, MLBJ, AW, IGM, JF, KSF, MM, CB, NB and LE participated in acquisition, analysis and interpretation of data; GLC, NB and LE drafted the manuscript; and GLC, MLBJ, AW, IGM, JF, KSF, MM, CB, NB and LE revised the manuscript critically for important intellectual content and approved the final version to be published. NB is the guarantor of this work.

References

1. Weir GC, Bonner-Weir S (2004) Five stages of evolving beta-cell dysfunction during progression to diabetes. Diabetes 53(Suppl 3): S16–S21
2. Butler AE, Janson J, Bonner-Weir S, Ritzel R, Rizza RA, Butler PC (2003) Beta-cell deficit and increased beta-cell apoptosis in humans with type 2 diabetes. Diabetes 52:102–110
3. Rahier J, Guiot Y, Goebbels RM, Sempoux C, Henquin JC (2008) Pancreatic beta-cell mass in European subjects with type 2 diabetes. Diabetes Obes Metab 10(Suppl 4):32–42
4. Bruun C, Christensen GL, Jacobsen ML et al (2014) Inhibition of beta cell growth and function by bone morphogenetic proteins. Diabetologia 57:2546–2554
5. Sanvito F, Herrera PL, Huarte J et al (1994) TGF-beta 1 influences the relative development of the exocrine and endocrine pancreas in vitro. Development 120:3451–3462
6. Smart NG, Apelqvist AA, Gu X et al (2006) Conditional expression of Smad7 in pancreatic beta cells disrupts TGF-beta signaling and induces reversible diabetes mellitus. PLoS Biol 4:e39
7. Yamaoka T, Idehara C, Yano M et al (1998) Hypoplasia of pancreatic islets in transgenic mice expressing activin receptor mutants. J Clin Invest 102:294–301
8. Ahnfelt-Ronne J, Ravassard P, Pardanaud-Glavieux C, Scharfmann R, Serup P (2010) Mesenchymal bone morphogenetic protein signaling is required for normal pancreas development. Diabetes 59: 1948–1956
9. Kumar M, Jordan N, Melton D, Grapin-Botton A (2003) Signals from lateral plate mesoderm instruct endoderm toward a pancreatic fate. Dev Biol 259:109–122
10. Sui L, Geens M, Sermon K, Bouwens L, Mfopou JK (2013) Role of BMP signaling in pancreatic progenitor differentiation from human embryonic stem cells. Stem Cell Rev 9:569–577
11. Hogan BL (1996) Bone morphogenetic proteins in development. Curr Opin Genet Dev 6:432–438
12. Little SC, Mullins MC (2006) Extracellular modulation of BMP activity in patterning the dorsoventral axis. Birth Defects Res C Embryo Today Rev 78:224–242
13. Kim MK, Jang EH, Hong OK et al (2013) Changes in serum levels of bone morphogenic protein 4 and inflammatory cytokines after bariatric surgery in severely obese Korean patients with type 2 diabetes. Int J Endocrinol 2013:681205
14. Koga M, Engberding N, Dikalova AE et al (2013) The bone morphogenic protein inhibitor, noggin, reduces glycemia and vascular inflammation in db/db mice. Am J Physiol Heart Circ Physiol 305: H747–H755
15. Bostrom KI, Jumabay M, Matveyenko A, Nicholas SB, Yao Y (2011) Activation of vascular bone morphogenetic protein signaling in diabetes mellitus. Circ Res 108:446–457
16. Goulley J, Dahl U, Baeza N, Mishina Y, Edlund H (2007) BMP4-BMPR1A signaling in beta cells is required for and augments glucose-stimulated insulin secretion. Cell Metab 5:207–219
17. Akerfeldt MC, Laybutt DR (2011) Inhibition of Id1 augments insulin secretion and protects against high-fat diet-induced glucose intolerance. Diabetes 60:2506–2514
18. Tominaga T, Abe H, Ueda O et al (2011) Activation of bone morphogenetic protein 4 signaling leads to glomerulosclerosis that mimics diabetic nephropathy. J Biol Chem 286:20109–20116
19. Koga M, Yamauchi A, Kanaoka Y et al (2013) BMP4 is increased in the aortas of diabetic ApoE knockout mice and enhances uptake of oxidized low density lipoprotein into peritoneal macrophages. J Inflamm 10:32
20. Brunstedt J (1980) Rapid isolation of functionally intact pancreatic islets from mice and rats by percollTM gradient centrifugation. Diabete Metab 6:87–89
21. Eliasson L, Ma X, Renstrom E et al (2003) SUR1 regulates PKA-independent cAMP-induced granule priming in mouse pancreatic B cells. J Gen Physiol 121:181–197
22. Airaksinen MS, Eilers J, Garaschuk O, Thoenen H, Konnerth A, Meyer M (1997) Ataxia and altered dendritic calcium signaling in mice carrying a targeted null mutation of the calbindin D28k gene. Proc Natl Acad Sci U S A 94:1488–1493
23. Frobose H, Ronn SG, Heding PE et al (2006) Suppressor of cytokine Signaling-3 inhibits interleukin-1 signaling by targeting the TRAF-6/TAK1 complex. Mol Endocrinol 20:1587–1596
24. Gopel S, Kanno T, Barg S, Galvanovskis J, Rorsman P (1999) Voltage-gated and resting membrane currents recorded from B cells in intact mouse pancreatic islets. J Physiol 521(Pt 3):717–728
25. Gopel SO, Kanno T, Barg S, Weng XG, Gromada J, Rorsman P (2000) Regulation of glucagon release in mouse-cells by KATP channels and inactivation of TTX-sensitive Na+channels. J Physiol 528:509–520
26. Ammala C, Eliasson L, Bokvist K, Larsson O, Ashcroft FM, Rorsman P (1993) Exocytosis elicited by action potentials and voltage-clamp calcium currents in individual mouse pancreatic B cells. J Physiol 472:665–688
27. Sooy K, Schermerhorn T, Noda M et al (1999) Calbindin-D(28 k) controls [Ca(2+)](i) and insulin release. Evidence obtained from calbindin-d(28 k) knockout mice and beta cell lines. J Biol Chem 274:34343–34349
28. Parkash J, Chaudhry MA, Amer AS, Christakos S, Rhoten WB (2002) Intracellular calcium ion response to glucose in beta-cells of calbindin-D28k nullmutant mice and in betaHC13 cells overexpressing calbindin-D28k. Endocrine 18:221–229
29. Lee D, Obukhov AG, Shen Q et al (2006) Calbindin-D28k decreases L-type calcium channel activity and modulates intracellular calcium homeostasis in response to K+ depolarization in a rat beta cell line RINr1046–38. Cell Calcium 39:475–485
30. Rorsman P, Braun M (2013) Regulation of insulin secretion in human pancreatic islets. Annu Rev Physiol 75:155–179
31. Eliasson L, Abdulkader F, Braun M, Galvanovskis J, Hoppa MB, Rorsman P (2008) Novel aspects of the molecular mechanisms controlling insulin secretion. J Physiol 586:3313–3324
32. Bazwinsky-Wutschke I, Wolgast S, Muhlbauer E, Peschke E (2010) Distribution patterns of calcium-binding proteins in pancreatic tissue of non-diabetic as well as type 2 diabetic rats and in rat insulinoma beta-cells (INS-1). Histochem Cell Biol 134:115–127
33. Keller MP, Choi Y, Wang P et al (2008) A gene expression network model of type 2 diabetes links cell cycle regulation in islets with diabetes susceptibility. Genome Res 18:706–716